SAND97-1936C
SAND--97-1936C
CONF-980528--

SEGREGATION GETTERING BY IMPLANTATION-FORMED CAVITIES AND B-Si PRECIPITATES IN SILICON

S.M. Myers, G.A. Petersen, D.M. Follstaedt, C.H. Seager, T.J. Headley, and J.R. Michael
Sandia National Laboratories, Albuquerque, New Mexico 87185-1056

W. Deweerd, G. Koops, J. Verheyden and H. Pattyn
Katholieke Universiteit Leuven, Instituut voor Kern- en Stralingfysika, B-3001 Leuven, Belgium

We show that Fe, Co, Cu, and Au in Si undergo strong segregation gettering to cavities and B-Si precipitates formed by He or B ion implantation and annealing. The respective mechanisms are argued to be chemisorption on the cavity walls and occupation of solution sites within the disordered, B-rich, B-Si phase. The strengths of the reactions are evaluated, enabling prediction of gettering performance.

RECEIVED
JAN 29 1998
OSTI

INTRODUCTION

We have examined the binding of transition metals to two types of gettering sink introduced into Si by ion implantation: cavities formed by He ion implantation and annealing, whose reactive internal surfaces are sites for chemisorption and metal-silicide precipitation; and disordered B-rich precipitates formed by implantation of B to supersaturation and annealing, where evidence points to solution of metal atoms at defect sites within the precipitated phase. Both of these sinks exhibit strong gettering of the metal solutes that were investigated, namely, Fe, Co, Cu, and Au. Moreover, the gettering mechanisms are of segregation type, and so remain active for solution concentrations below the metal solubilities. We investigated the mechanisms and energetics using several experimental approaches, and our findings are summarized in this paper. Certain aspects of the work are treated in greater detail elsewhere (1-4). It should be noted that numerous other workers have also reported the occurrence of transition-metal gettering at cavities, as cited in Refs. 1-4. In the present, abbreviated discussion, we refer to this literature selectively as it bears on particular points.

FORMATION AND MICROSTRUCTURE OF THE GETTERING SINKS

Ion implantation of He into Si at room temperature produces bubbles when the concentration exceeds ~1.6 at.%. Subsequent annealing at temperatures $\gtrsim$700°C causes diffusion of the He from the material, leaving a buried layer of faceted voids that remains at temperatures approaching 1200°C [5,6]. A representative microstructure, observed by cross-section transmission electron microscopy (XTEM), is shown in Fig. 1. Cavity layers of this kind have been created at depths as large as 5 μm using MeV implantation energies, with the overlying Si remaining sufficiently free of electrically active defects to

DISCLAIMER

accommodate deep-level transient spectroscopy (DLTS) of residual Fe in solution [7]. The cavity walls themselves are electrically active, and hence should be separated from the device region by more than the Debye carrier-screening length [8].

When Si is supersaturated with B at elevated temperatures, the necessary density being $\sim 10^{20}$ atoms/cm^3, there is precipitation of a B-rich phase. According to a published phase diagram [9], thermodynamic equilibrium at temperatures $\lesssim 1270°C$ should to give rise to a complex, rhombohedral phase of approximate composition B_3Si containing icosahedral structural units. In fact, in an earlier study where Si doped with 3×10^{20} B/cm^{-3} during growth was annealed at 1100°C for 240 hours, micrometer-size precipitates were observed having an electron diffraction pattern consistent with the above phase [10]. In contrast, when the B is introduced by ion implantation at room temperature, resulting in defect-enhanced diffusion and presumably a high density of damage-related nucleation sites during subsequent annealing, we find that the precipitates have much smaller size, ~10 nm, and that long range structural order is not achieved even after 24 hours at 1200°C. A high-resolution, [110] Si phase-contrast TEM image of a precipitate formed at 1100°C is shown in Fig. 2, where the absence of long-range order in the particle is reflected by the irregular granularity of its image. Electron-energy-loss spectroscopy (EELS) using a 1 nm beam indicates that the composition of the particle is B_xSi with $x \gtrsim 2$. The chemical potential of B in the disordered precipitated phase, as deduced from the equilibrated concentration of B in solution in the adjacent Si lattice, is not resolvably different from that reported for crystalline B_3Si [3]. From these findings we infer that the disordered B-Si phase probably has local bonding and structure similar to that of crystalline B_3Si, and that the development of long-range structural order is retarded by the small associated change in free energy and possibly by the small size of the particles.

GETTERING MECHANISMS

The walls of cavities within Si are chemically reactive as a result of dangling orbitals. These internal surfaces can be expected to accommodate chemisorption of transition-metal solutes and also, when the metal concentration in the adjacent Si lattice exceeds the thermodynamic solubility, precipitation of three-dimensional metal silicides. Such behavior was confirmed in experiments with Cu and Au solutes. In particular, when we introduced cavities into Si after the solution concentration of Cu or Au was stabilized at the solubility by prior formation of the metal-silicide phase, metal atoms accumulated on the cavity walls until a coverage of about 1 monolayer (ML) was reached, whereupon the gettering abruptly ceased [1,4]. This is illustrated by the results for Au shown in Fig. 3, which were obtained by concentration profiling with Rutherford backscattering spectrometry (RBS); here the slight decrease in the saturation areal density with increasing temperature reflects a gradual agglomeration of the cavities and a resultant reduction in total wall area. Moreover, TEM of the Cu-saturated cavities showed no evidence of precipitation within the open volumes [1]. In contrast, when other investigators implanted Cu or Au into the vicinity of cavities without prior silicide precipitation and the material was then annealed, conditions under which local supersaturation is reasonably anticipated, precipitation within the voids was evident in TEM micrographs [11,12]. Iron and Co are also gettered from their respective metal silicides to chemisorption sites on cavity walls, albeit at coverages less than 1 ML due to the relatively high stabilities of $FeSi_2$ and $CoSi_2$, as will be discussed in the following section. The local environment of Co atoms gettered to cavities has been examined by some of us using Mössbauer spectroscopy of ^{57}Co; the observed spectrum has pronounced quadrupole splitting indicative of a non-cubic site, and it is distinct from the spectrum of $CoSi_2$ or of other recognized sites of Co within Si, consistent with a wall-chemisorption mechanism [13]. Finally, recent experiments where Cu was gettered from internal metal-silicide precipitates to clean external (111) and (100) surfaces in ultrahigh vacuum (UHV) showed that the (111) surface getters substantially more effectively that (100) [14]. The (111) surface is also the most stable on Si, and as a result it is the dominant facet of the cavities [15,16].

Our experiments show that Fe, Co, Cu, and Au are gettered by the disordered B-Si precipitates discussed in the preceding section [3]. Cobalt concentration profiles obtained by secondary ion mass spectrometry (SIMS) that exhibit this effect are shown in Fig. 4. Here, $CoSi_2$ was first formed in great excess on the back sides of two wafers by Co ion implantation and annealing, as described elsewhere [2], thereby pinning the solution concentration at the solubility. Boron was then implanted on the front side, in one case to supersaturation and the other case not, and the specimens were annealed at 900°C to induce B-Si precipitation and gettering. The depth profiles in Fig. 4 show substantial gettering of Co from the silicide phase to the region containing B-Si precipitates within the initially B-supersaturated specimen; the location of these precipitates corresponds to the indicated bump in the B profile. There is much less accumulation of Co in the regions continuing only substitutional B, indicating that the B–Co pairing reaction produces weaker binding; this finding was replicated for all of the investigated metals.

Detailed profiling studies also indicate that, for each of the metals, the number of metal atoms gettered at a given temperature is proportional to the number of precipitated B atoms when the metal concentration in the surrounding Si lattice is held at the solubility by remote, excess metal silicide. Moreover, for a given temperature and given number of precipitated B atoms, the number of gettered Fe atoms scales with the residual concentration of ungettered Fe in the Si as measured by deep level transient spectroscopy (DLTS). This proportionality is seen in Fig. 5. Here, Fe concentrations below the solubility were studied in samples not containing the concentration-pinning metal-silicide phase. These two proportionalities are consistent with a gettering mechanism whereby the metal atoms segregate exothermically from solution in Si to solution sites within the disordered B-Si precipitated phase.

The nature of the metal site in the disordered B-Si phase is elucidated by Mössbauer spectroscopy of ^{57}Co gettered at 900°C, whose spectrum is shown in Fig. 6. The quadrupole splitting indicates a substantial departure from cubic symmetry. Moreover, the large difference between this spectrum and that of Co within $CoSi_2$, also shown, demonstrates that metal-silicide formation does not play a role in the gettering. The spectrum of Co ion-implanted into bulk, crystalline B_3Si at room temperature is very similar to that of the gettered atoms, as seen in the figure; but, strikingly, annealing of this bulk sample at 900°C resulted in a quite different spectrum corresponding to cubic $CoSi_2$. Our tentative interpretation is that the accommodation of the metal atoms in atomic solution within the B-Si phases requires defects, which are present in the structurally disordered precipitates and also in the room-temperature-implanted crystalline B_3Si, but not in the latter material after annealing.

STRENGTHS OF THE GETTERING REACTIONS

A relatively direct method of determining the strength of a gettering reaction is to measure, under equilibrium conditions, the number of metal atoms in the sinks as a function of the residual concentration of metal atoms in solution in the nearby Si lattice. If this were done for all temperatures and concentrations of interest, and in the absence of significant activation barriers to the reaction, no additional information would be needed to predict gettering performance. In practice, however, such a procedure is difficult due to the large parameter space and the challenge of measuring the small relevant solution concentrations of some of the metals. To make the characterization more tractable, we have taken two steps. First, the gettering reactions are described by simplified physical models, whose parameters can be extracted from a smaller body of experimental information. Second, the reactions were mostly examined by experimental methods less direct but more readily carried out than the simultaneous measurement of trapped quantity and residual solution concentration, which was done in only a few instances as a check. This approach is expeditious, and we believe that it has yielded a valid semiquantitative indication of the gettering strengths of cavities and B-Si precipitates that can be used for realistic prediction of gettering performance under device-relevant conditions. In the remainder of this section, we first present the simplified mathematical models and then discuss the experiments used to extract their parameters.

As discussed in the preceding section, gettered metal atoms are inferred to occupy chemisorption sites on cavity walls and solution sites within the disordered B-Si precipitates. With the simplifying assumptions that there is a single type of saturable binding site in each case and that these sites act independently of one other, the equilibrium concentration of metal atoms remaining in solution is given by

$$[\mathrm{M,soln}] = \{\theta/(1-\theta)\}\exp(-\Delta G/kT)\,. \qquad [1]$$

Here [M,soln] is in atomic fraction, θ is the fraction of binding sites that are occupied, and ΔG is a temperature-dependent binding free energy defined as

$$\Delta G = \Delta H - T\Delta S_{ex} \qquad [2]$$

with ΔH being the enthalpy change between bound states and interstitial solution in Si and ΔS_{ex} the excess, nonconfigurational part of the entropy difference. In the event of a two-phase condition on the cavity walls at higher occupancies, such as ordered adsorbate islands coexisting with random chemisorption or metal silicides coexisting with chemisorption, Eq. [1] is replaced by

$$[M,soln] = \exp(-\Delta G/kT) \quad [3]$$

with a different value of ΔG. Equations [1] and [3] define the boundary conditions that are assumed to exist at the margins of the gettering sinks.

Utilization of Eq. [1] requires knowledge of the total number of trap sites in order for the fractional occupation θ to be calculated from the measured number of gettered metal atoms. In the case of cavities, the number of available wall sites has been evaluated from micrographs and verified by measuring saturation levels for Cu and Au; an example of such saturation is seen in Fig. 3. In contrast, the density of metal solution sites within the disordered B-Si phase is not known. To treat this case, we recast Eq. [1] as

$$[M,soln] \simeq \alpha\{[M,BSi]/[B,BSi]\}\exp(-Q/kT)\,. \quad [1a]$$

Here the braces contain the ratio of metal atoms to B atoms within the B-Si phase, which is proportional to θ, Q is an empirical activation energy $\simeq\Delta H$, and α is a constant of proportionality. Equation [1a] is applicable for $\theta << 1$.

Two experimental methods not requiring the actual measurement of solution concentrations were used to characterize the strengths of the gettering centers. In the first approach, the sinks were allowed to come into equilibrium with a substantial excess of metal-silicide phase located at a different depth within the wafer. These silicides were formed by ion-implanting the metal to a concentration of several at.% and then annealing; actual formation of the phases was assured either by transmission electron diffraction or by replicating formation conditions reported in the literature [1,2,4]. Then, when the solubility of the metal in Si in equilibrium with the silicide phase is well known, as for Fe and Co, the value of [M,soln] in Eqs. [1], [3], and [1a] can be equated to that solubility. With this information, measurement of the number of gettered metal atoms by depth profiling served to determine the parameters in the equations. This approach was used for gettering of Fe and Co at cavities, and the resulting values of ΔG are among those plotted in Fig. 7. Metal-silicide binding energies for Fe and Co taken from the literature [17] are included for comparison.

Analogous experiments were carried out to examine gettering by B-Si precipitates; the measured concentration of metal atoms within the B-Si phase under conditions of equilibrium with remote metal silicide is shown in Fig. 8 for Fe, Co, Cu, and Au. In the particularly important case of Fe, the relatively small size of the gettered concentration leads us to believe that the gettering sites are far from saturation and that Eq. [1a] is therefore applicable. This belief is reinforced by the near proportionality between [M,soln] and [M,BSi]/[B,BSi] seen in Fig. 5. Consequently, the segregation of Fe from solution in Si to solution within the B-Si phase can be characterized in terms of a concentration ratio dependent only on temperature. This ratio was extracted from Fig. 8 and is shown in Fig. 9.

The above approach was not applicable to the trapping of Cu and Au at cavities because, under conditions of equilibrium with the metal-silicide phase, θ was found to be

$\simeq 1$, corresponding to trap saturation. Such saturation indicates only that the metal is bound to wall-chemisorption sites at least as strongly as in the metal silicide. To obtain more quantitative information, we employed a second method in which RBS was used to measure the rates of Cu and Au redistribution between two cavity layers, one of these (#1) initially containing metal atoms and the other (#2) initially unoccupied. The essential concept of the experiment is that, so long as $\theta_2 < \theta_1$ and θ_2 is sufficiently small for Eq. [1] to be applicable, $[M,soln]_2 < [M,soln]_1$, and the resulting concentration gradient causes diffusion of metal atoms from layer 1 to layer 2. Assuming near-steady-state diffusion between gettering layers of negligible width that are separated by ΔX, the diffusion flux is given by

$$\Phi \simeq N_{Si} \{ [M,soln]_1 - [M,soln]_2 \} D_M / \Delta X \qquad [4]$$

where N_{Si} is the atomic density of Si and D_M is the metal diffusion coefficient. Appropriate substitution for the [M,soln] from Eqs. [1] and [3] then relates the measured interlayer flux to ΔG, allowing this quantity to be evaluated. In practice, the analysis of data was accomplished by solving the diffusion problem numerically [1,4] rather than using the approximate relationship of Eq. [4]. Moreover, in the case of Au, the consequences of the metal atoms occupying substitutional as well as interstitial sites within the Si lattice were taken into account [4]. Figure 10 shows representative data and theoretical fits from such experiments on Au in Si. In a variation of this approach, the diffusive flux of metal atoms from a layer containing silicide phase to a layer of cavity traps was also measured, permitting the binding free energy within the silicide phase to be extracted for Cu and Au. Representative data and theoretical fits are shown in Fig. 3 for the case of Au. Results are in satisfactory agreement with published information on the respective solubilities, as discussed elsewhere [1,4]. The various cavity and silicide binding free energies obtained for Cu and Au from these interlayer-redistribution experiments are included in Fig. 7. In the case of Au, the effective binding free energy was found to vary slightly as a function of wall coverage [4]; the values shown in Fig. 7 correspond to the highest coverage levels.

It is noteworthy in Fig. 7 that the difference between the cavity binding free energy and the silicide binding free energy changes from positive to negative on going from monovalent Cu and Au to multivalent Fe and Co. This can be qualitatively interpreted as arising from the difficulty of achieving high bonding coordination numbers on the Si surface [18]. In particular, Cu and Au atoms satisfy their bonding needs by reacting with a single dangling orbital while simultaneously providing energy-reducing passivation of the Si surfaces. As a result, chemisorption is preferred over silicide formation. In the contrasting cases of Fe and Co, the requisite large number of metal bonds is present in the disilicide phases, where the coordination number is 8, but is not readily achieved by chemisorption. As a result, ΔG is greater for the silicides.

CONCLUSIONS AND IMPLICATIONS

In this study we demonstrated that cavities and disordered B-Si precipitates are effective gettering sinks for Fe, Co, Cu, and Au in Si. Mechanisms were proposed based on a variety of experimental evidence. Moreover, by applying simplified mathematical models to specially designed experiments, we evaluated the strengths of the gettering reactions. The result is a general capability for prediction of gettering performance whose accuracy is believed to range from semiquantitative to quantitative. Recent studies of Fe gettering by cavities in competition with internal gettering by SiO_2 precipitates, where comparison was made with model predictions, are in accord with this assessment [7].

Further studies of these reactions are nonetheless needed. In the case of cavities, the provisional simplifications embodied in Eqs. [1] and [3] contrast with the complex behaviors of transition metals on Si surfaces that have been observed in UHV studies of external surfaces, where multiple ordered chemisorption states can arise [19]. Even in the regime of low cavity-wall coverage, Mössbauer spectroscopy of gettered ^{57}Co has evidenced two types of gettering site with different binding energies [13]. In this situation, it is desirable to advance from the simplified description of Eqs. [1] and [3] toward a more complete determination of the general relationship $[M,soln] = f(\theta,T)$. As for gettering by B-Si precipitates, the information reported herein for Fe suggests that Eq. [1] may in fact be fairly accurate for this metal, at least at lower occupancies. It is premature to assert this as a general conclusion for all of the metals and all occupancies, however. Furthermore, the density of trap sites within the disordered B-Si phase is still to be determined. Also outstanding is the question of whether the crystalline form of B-Si accommodates the exothermic incorporation of transition-metal atoms as does the disordered phase. In addition to its scientific significance, this issue may influence whether B-Si gettering can be implemented by growing B into the Si instead of implanting it.

Several properties of the cavity and B-Si sinks are noteworthy in connection with their potential use for gettering. First, the binding reactions are relatively strong: the binding free energies for cavities shown in Fig. 7 fall within the approximate range 1.4-2.5 eV for elevated temperatures relevant to gettering, while the segregation ratio for Fe in the B-Si phase shown in Fig. 9 has an activation energy of 2.3 eV and remains above 10^4 at 1100°C. Of comparable significance is the fact these gettering reactions are of segregation type, and so are expected to remain active at arbitrarily small impurity levels. This is in contrast to mechanisms based on metal-silicide precipitation such as internal gettering [20], which are inoperative at concentrations below the solid solubility. As a consequence of these properties, the cavities and B-Si precipitates are predicted to reduce the concentrations of metals in solution by relatively large factors at relatively high temperatures, and to do this in wafers of arbitrarily high starting purity. Furthermore, by reducing metal solution concentrations below the solubility, these new sinks should serve to induce dissolution of metal-silicide particles at undesirable locations.

Another significant consideration is that the introduction of cavities and B-Si precipitates into the device side of the wafer appears probably feasible, through implantation to sufficient depths using appropriately high beam energies, or through Si epitaxial growth after the sinks are formed. Since, in addition, the traps in these gettering layers are sufficiently dense to act as a virtually continuous planar sink, gettering diffusion lengths should be reduced to the micrometer range. This means that gettering can be carried out at relatively low temperatures where the effectiveness of all sinks are enhanced.

Figure 11 shows modeling results that illustrate the expected gettering behavior of Si-B precipitates and reinforce several of the points made above. In this calculation, a wafer of thickness 0.5 mm was assumed to contain initially a uniform Fe solution concentration of 1×10^{12} cm^{-3}. The metal solute was gettered at 700°C by one of two processes: 1) segregation to B-Si precipitates within a 0.2-μm layer centered 5 μm beneath the surface containing 1×10^{17} B/cm^2; or 2) $FeSi_2$ precipitation at SiO_2 particles distributed through the bulk with a density-radius product of 4.8×10^5cm^{-2} (as in Ref. 20) and a depletion layer extending from the surface to 10 μm ("internal gettering"). The evolution of the system was treated by numerically solving diffusion-reaction equations discussed elsewhere [1], with the strength of the B-Si sinks being taken from Fig. 9. Plotted in the figure for the two cases is the near-surface Fe concentration as a function of gettering time. In the case of internal gettering by SiO_2 particles, the solution concentration is reduced to the thermodynamic solubility [17] on a time scale determined by diffusion kinetics. The segregation gettering to B-Si precipitates exhibits two stages: first, within a few seconds, a diffusion-controlled approach to equilibrium between sinks and solution in the near-surface region reduces the near-surface concentration from 10^{12} to $\sim10^7$ Fe/cm^3; then, at times $\gtrsim10^3$ s, Fe from the underlying bulk further populates the sinks, with a resultant increase in the equilibrium solution concentration in accord with Eq. [1a].

ACKNOWLEDGMENT

This work was supported by the U. S. Dept. of Energy, Office of Basic Energy Sciences, under Contract DE-AC04-94AL85000. Sandia National Laboratories is a multiprogram laboratory operated by Sandia Corporation, a Lockheed Martin Company, for the U. S. Dept. of Energy.

REFERENCES

1. S. M. Myers and D. M. Follstaedt, J. Appl. Phys. **79**, 1337 (1996).
2. S. M. Myers, G. A. Petersen, and C. H. Seager, J. Appl. Phys. **80**, 3717 (1996).
3. S. M. Myers, G. A. Petersen, T. J. Headley, J. R. Michael, T. L. Aselage, and C. H. Seager, Nucl. Instrum. Methods B **127-128**, 291 (1997).
4. S. M. Myers and G. A. Petersen, Phys. Rev. B, 1998, in press.

5. C. C. Griffioen, J. H. Evans, P. C. De Jong, and A. Van Veen, Nucl. Instrum. Methods B **27**, 417 (1987).
6. D. M. Follstaedt, S. M. Myers, G. A. Petersen, and J. W. Medernach, J. Electronic Materials **25**, 151 (1996).
7. S. A. McHugo, E. R. Weber, S. M. Myers, and G. A. Petersen, J. Electrochem. Soc., 1998, in press.
8. C. H. Seager, S. M. Myers, R. A. Anderson, W. L. Warren, and D. M. Follstaedt, Phys. Rev. B **50**, 2458 (1994).
9. R. W. Olesinski and G. J. Abbaschian, Bull. Alloy Phase Diagrams **5**, 478 (1984).
10. A. Armigliato, D. Nobili, P. Ostoja, M. Servidori, and S. Solmi, in Semiconductor Silicon, H. R. Huff and E. Sirtl, Editors, pp. 638-647, Electrochemical Soc., Pennington, NJ, (1977).
11. J. Wong-Leung, C. E. Ascheron, M. Petravic, R. G. Elliman, and J. S. Williams, Appl. Phys. Lett. **66**, 1231 (1995).
12. J. Wong-Leung, J. S. Williams, and E. Nygren, Nucl. Instrum Methods B **106**, 424 (1995).
13. W. Deweerd, T. Barancira, S. Bukshpan, S. Demuynck, G. Langouche, K. Milants, R. Moons, J. Verheyden, and H. Pattyn, Phys. Rev. B **53**, 16637 (1996).
14. W. R. Wampler, Mat. Res. Soc. Symp. Proc. **448**, 371 (1997).
15. D. M. Follstaedt, Appl. Phys. Lett. **62**, 1116 (1993).
16. D. J. Eaglesham, A. E. White, L. C. Feldman, N. Moriya, and D. C. Jacobson, Phys. Rev. Lett. **70**, 1643 (1993).
17. E. R. Weber, Appl. Phys. A **30**, 1 (1983), and citations therein.
18. P. J. Feibelman, private communication.
19. See, e.g., the discussion of Au on Si(111) by R. Plass and L. D. Marks, Sur. Sci. **380**, 497 (1997).
20. D. Gilles, E. R. Weber, and S.-K. Hahn, Phys. Rev. Lett. **64**, 196 (1990).

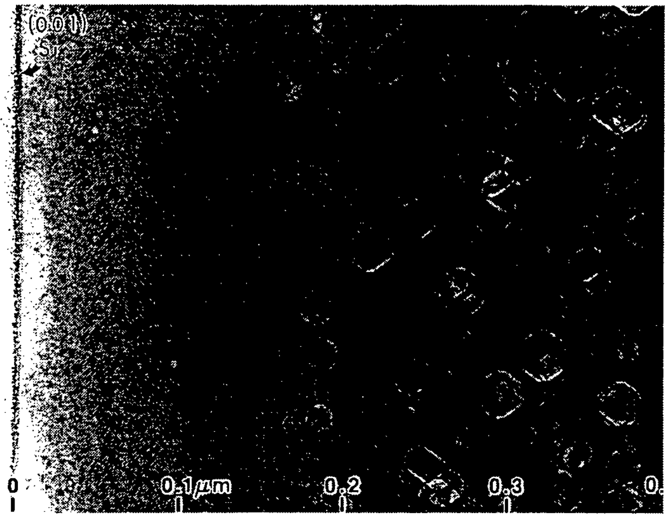

Fig. 1. XTEM of cavities in Si formed by implanting 10^{17} He/cm^2 at 30 keV and vacuum annealing at 900°C for 1 hour.

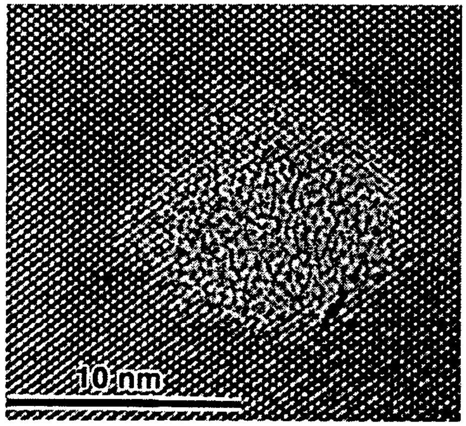

Fig. 2. [110] Si phase-contrast image of B-Si precipitate in Si formed at 1100°C.

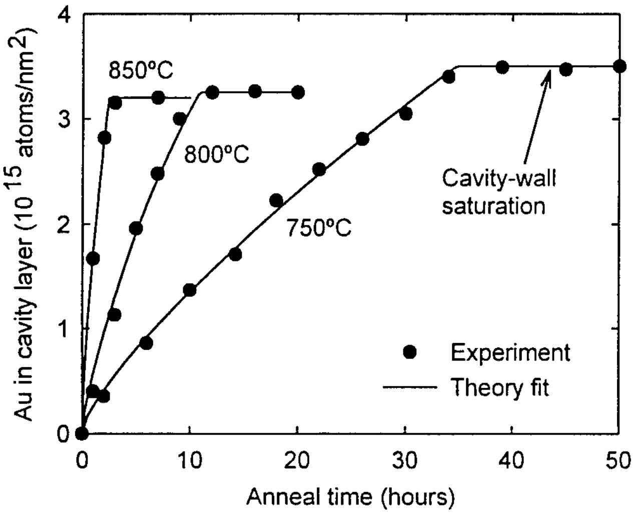

Fig. 3. Redistribution of Au from a layer with Au-Si phase to a cavity layer at three temperatures. The separation of the two layers is approximately 0.7 μm.

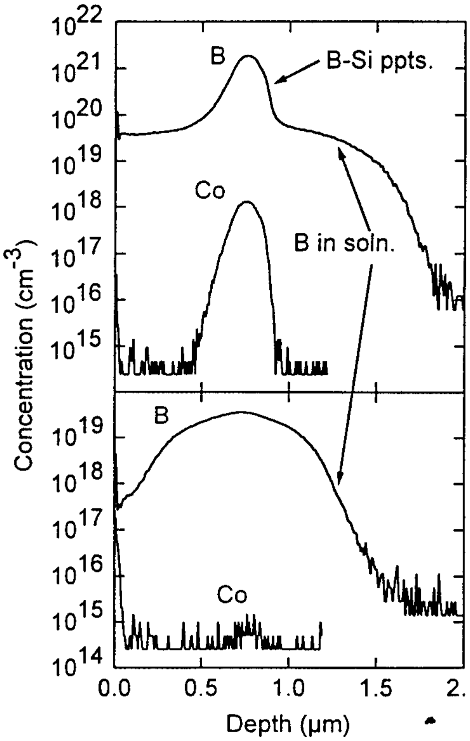

Fig. 4. Concentration profiles showing gettering of Co from a layer with $CoSi_2$ phase to a layer with B-Si precipitates. The $CoSi_2$ and B-Si layers are on opposite sides of the wafer.

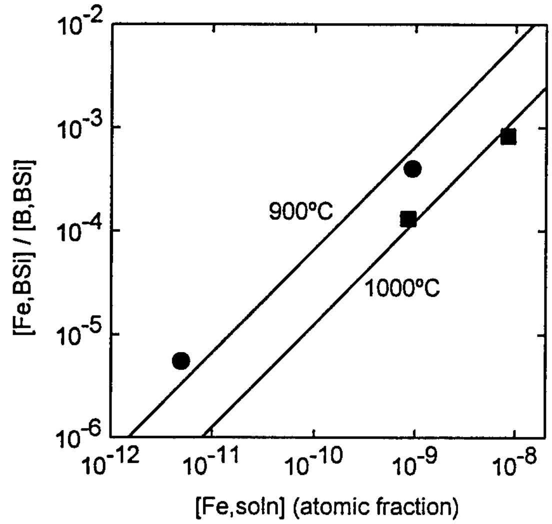

Fig. 5. Variation of the Fe content of B-Si precipitates as a function of the Fe concentration in solution in the Si lattice. The lines correspond to direct proportionality.

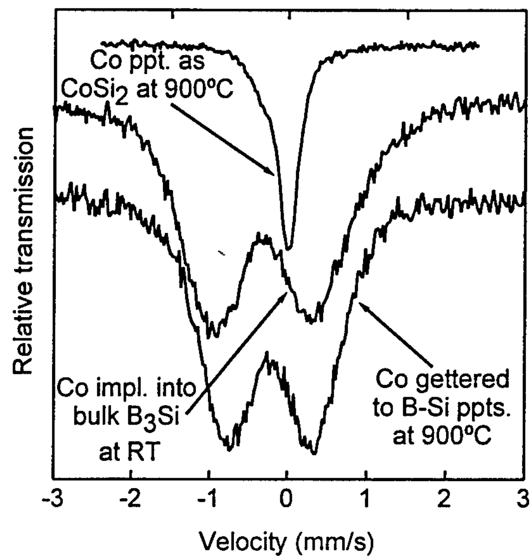

Fig. 6. Mössbauer spectra of ^{57}Co in B-Si precipitates and in related states.

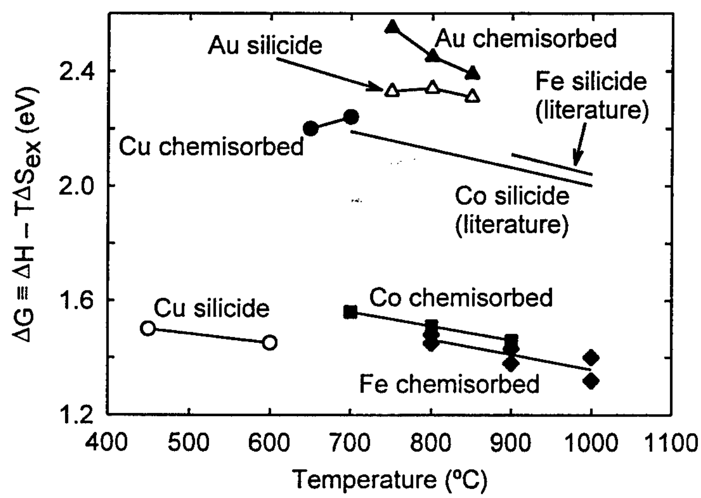

Fig. 7. Binding free energies of metals chemisorbed on cavity walls relative to solution in the Si lattice.

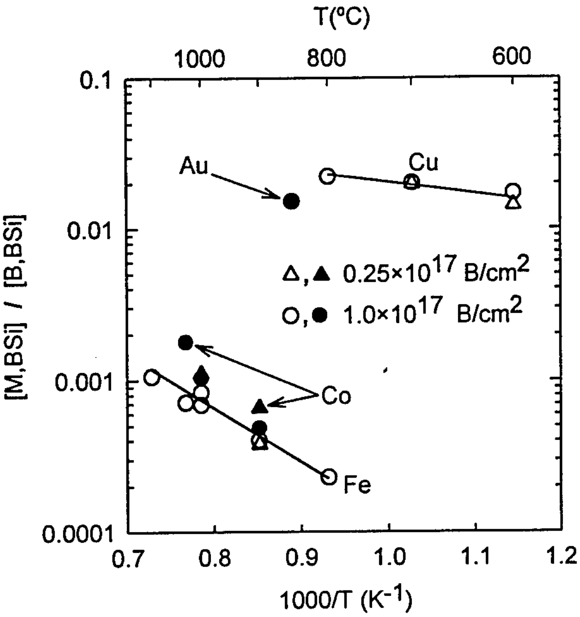

Fig. 8. Metal contents of B-Si precipitates in equilibrium with the respective metal silicide phases.

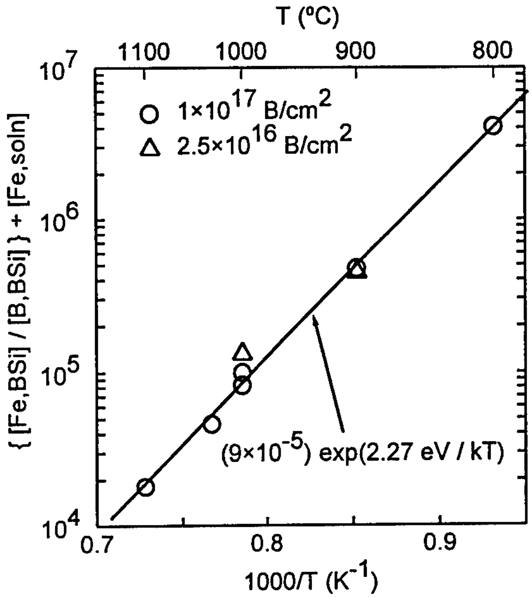

Fig. 9 Concentration ratio for the segregation of Fe from solution in Si to solution in the precipitated B-Si phase.

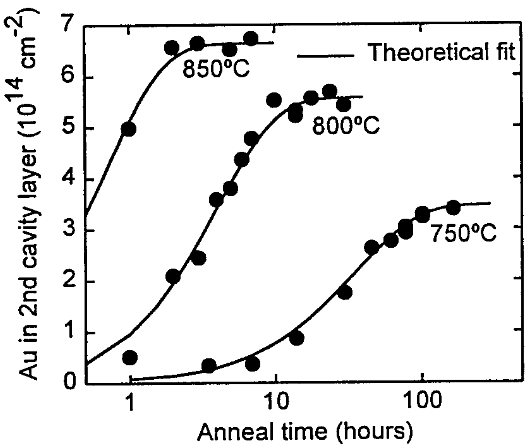

Fig. 10. Redistribution of Au from an initially occupied cavity layer to a second, initially unoccupied layer at three temperatures. The separation of the two layers is approximately 0.7 μm.

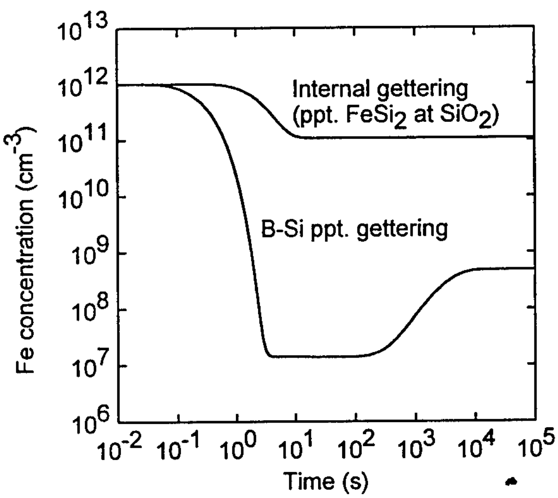

Fig. 11. Predicted variation of near-surface Fe concentration at 700°C during segregation gettering by B-Si precipitates at 5 μm or internal gettering by SiO_2 precipitates at >10 μm.

M98004109

Report Number (14) SAND-- 97-1936 C

CONF-980528--

Publ. Date (11) 199801

Sponsor Code (18) DOE/ER, XF

UC Category (19) UC-400, DOE/ER

DOE